International Journal of Cardiology xxx (xxxx) xxx

Contents lists available at ScienceDirect

International Journal of Cardiology

journal homepage: www.elsevier.com/locate/ijcard

Cardiovascular imaging modalities in the diagnosis and management of rheumatic heart disease

Olukayode O. Aremu [a], Petronella Samuels [c], Stephen Jermy [c,d], Evelyn N. Lumngwena [a,b,e,f], Daniel Mutithu [a,b], Blanche J. Cupido [a], Sebastian Skatulla [g,h], Ntobeko A.B. Ntusi [a,b,c,*]

[a] Division of Cardiology, Department of Medicine, University of Cape Town, Cape Town, South Africa
[b] Department of Medicine, Hatter Institute for Cardiovascular Research in Africa, University of Cape Town, Cape Town, South Africa
[c] Cape Universities Body Imaging Centre, Faculty of Health Sciences, University of Cape Town, South Africa
[d] Division of Biomedical Engineering, Department of Human Biology, University of Cape Town, Cape Town, South Africa
[e] Institute of Infectious Disease and Molecular Medicine, University of Cape Town, South Africa
[f] Centre for the Study of Emerging and Ee-emerging Infections (CREMER), Institute for Medical Research and Medicinal Plant studies (IMPM), Ministry of Scientific Research and Innovation, Cameroon
[g] Division of Structural Engineering and Mechanics, Department of Civil Engineering, University of Cape Town, South Africa
[h] Department of Civil Engineering, Centre for Research in Computational and Applied Mechanics (CERECAM), University of Cape Town, South Africa

ARTICLE INFO

Article history:
Received 22 April 2020
Received in revised form 9 July 2020
Accepted 20 September 2020
Available online xxxx

Keywords:
Rheumatic heart disease
Acute rheumatic fever
Echocardiography
Cardiovascular magnetic resonance
Computed tomography

ABSTRACT

Rheumatic heart disease (RHD) is prevalent in sub-Saharan Africa, where the capacity for diagnosis and evaluation of disease severity and complications is not always optimal. While the medical history and physical examination are important in the assessment of patients suspected to have RHD, cardiovascular imaging techniques are useful for confirmation of the diagnosis. Echocardiography is the workhorse modality for initial evaluation and diagnosis of RHD. Cardiovascular magnetic resonance is complementary and may provide additive information, including tissue characteristics, where echocardiography is inadequate or non-diagnostic. There is emerging evidence on the role of computed tomography, particularly following valve replacement surgery, in the monitoring and management of RHD. This article summarises the techniques used in imaging RHD patients, considers the evidence base for their utility, discusses their limitations and recognises the clinical contexts in which indications and imaging with various modalities are expanding.

1. Introduction

Rheumatic heart disease (RHD) refers to delayed cardiac damage caused by recurrent episodes of acute rheumatic fever (ARF) (abbreviations in Table 1) [1]. ARF is triggered by group A β-streptococcal (GAS) infection, primarily affecting the joints, skin, central nervous system and the heart [2]. RHD is the leading cause of acquired cardiovascular disease (CVD) in low- and middle-income countries (LMICs) [3,4], affecting 15–19 million people globally and resulting in over 230,000 deaths per annum. [5–7] ARF and RHD prevalence in LMICs is compounded by poverty, limited access to healthcare, and genetic susceptibility to GAS (Fig. 1) [4,8].

Cardiovascular imaging in RHD aids in assessment of cardiac structure and function, disease mechanism, severity and haemodynamic adaptations and ventricular remodeling [9,10]. Echocardiography, cardiovascular magnetic resonance (CMR) and computed tomography (CT) are variably employed in evaluating RHD. [11]

While transthoracic echocardiography (TTE) is the first-line imaging modality for the comprehensive evaluation of RHD, in patients with inadequate views or suspected complications, including infective endocarditis, transoesophageal echocardiography (TOE) is an ideal adjunctive technique and also helps on deciding on optimal timing of intervention [12]. Invasive coronary angiography or catheterisation is helpful for interventional procedure, right heart studies or planning concomitant coronary bypass surgery, whereas fluoroscopy is the mainstay technique for procedural guidance on ventricular remodeling and valvular function.

In this review, the role of current imaging modalities in the assessment of RHD is summarised. Each of the left-sided valve lesions, with the application of the imaging modalities is addressed in a separate section according to prevalence in LMICs.

* Corresponding author at: Department of Medicine, University of Cape Town and Groote Schuur Hospital, J46.53, Old Main Building, Groote Schuur Hospital, Main Road, Observatory, 7925, South Africa.
E-mail address: ntobeko.ntusi@uct.ac.za (N.A.B. Ntusi).

https://doi.org/10.1016/j.ijcard.2020.09.049
0167-5273/

Table 1
Abbreviations.

AHA/ACC	American Heart Association/American College of Cardiology
AR	Aortic regurgitation
ARF	Acute rheumatic fever
AS	Aortic stenosis
AV	Aortic valve
AVA	Aortic valve area
GAS	Group A streptococcus
CMR	Cardiovascular magnetic resonance
CT	Computed tomography
CVD	Cardiovascular disease
ECG	Electrocardiogram/electrocardiography
HIC	High-income countries
LA	Left atrium/atrial
LMICs	Low- and middle-income countries
LV	Left ventricle/ventricular
LVEF	Left ventricular ejection fraction
MR	Mitral regurgitation
MS	Mitral stenosis
MV	Mitral valve
MVA	Mitral valve area
PV	Pulmonary valve
RHD	Rheumatic heart disease
RV	Right ventricle/ventricular
SSFP	Steady state free precession
TOE	Transoesophageal echocardiography
TTE	Transthoracic echocardiography
TV	Tricuspid valve

2. Imaging techniques

2.1. Echocardiography

Echocardiography uses high frequency (2–10 MHz) sound waves to image cardiac structures and assess function. Two-dimensional (2D) TTE is the standard imaging modality for valvular lesions; it determines severity, quantifies haemodynamic outcomes, left atrial size, ventricular remodeling and pulmonary artery pressure [13,14]. 2D-echocardiography often reveals thickened, elongated chordae which may cause prolapse of the anterior mitral valve leaflet [3]. Echocardiography can detect number and thickness of cusps, calcification, sub- or supra-valvular stenosis and dilation of the ascending aorta/pulmonary trunk. Further, TTE is helpful in delineating components of the valvular apparatus including the annulus, cusps, chordae tendinae, papillary muscles and their attachments to the ventricular walls [15]. Further advantages include low cost, portability, accessibility and non-ionising radiation [16]. Echocardiography, however, is highly operator-dependent and limited by specific acoustic windows, comorbid disease and altered physiology. CMR and CT may be helpful in cases of ambiguous echocardiography and/or conflicting clinical findings [17].

2.2. Cardiovascular magnetic resonance

CMR is a robust imaging modality, free of ionising radiation, with high spatial and temporal resolution, performed via excitation of hydrogen protons within a static magnetic field. The magnetic field aligns the nuclear magnetisation spins of the hydrogen protons, which are then excited by radiofrequency (RF) pulses. After the RF pulses are switched off, the protons dissipate energy as they precess back to their equilibrium magnetisation. This dissipated energy is detected by receiver coils and Fourier transformation is used to convert frequencies into images [18]. CMR usually involves electrocardiographic (ECG)-vector gating and breath-hold acquisitions to circumvent artefacts. Balanced steady-state free precession (SSFP) sequences are applied in the short-axis plane and in 2-, 3-, and 4-chamber planes to allow morphologic assessment chamber structure, wall motion and extent of valvular regurgitation.

Contrast-enhanced CMR offers the capability to directly discriminate fibrotic or infarcted tissue from normal myocardium and indicates the severity and extent of myocardial injury [18]. Similar to cine CMR, tagging may be acquired to assess cardiac motion and deformation; and provides more direct and accurate quantification of regional motion and strain. Velocity-encoded phase contrast CMR allows a direct visual assessment of signal void created by the regurgitant jet, which gives

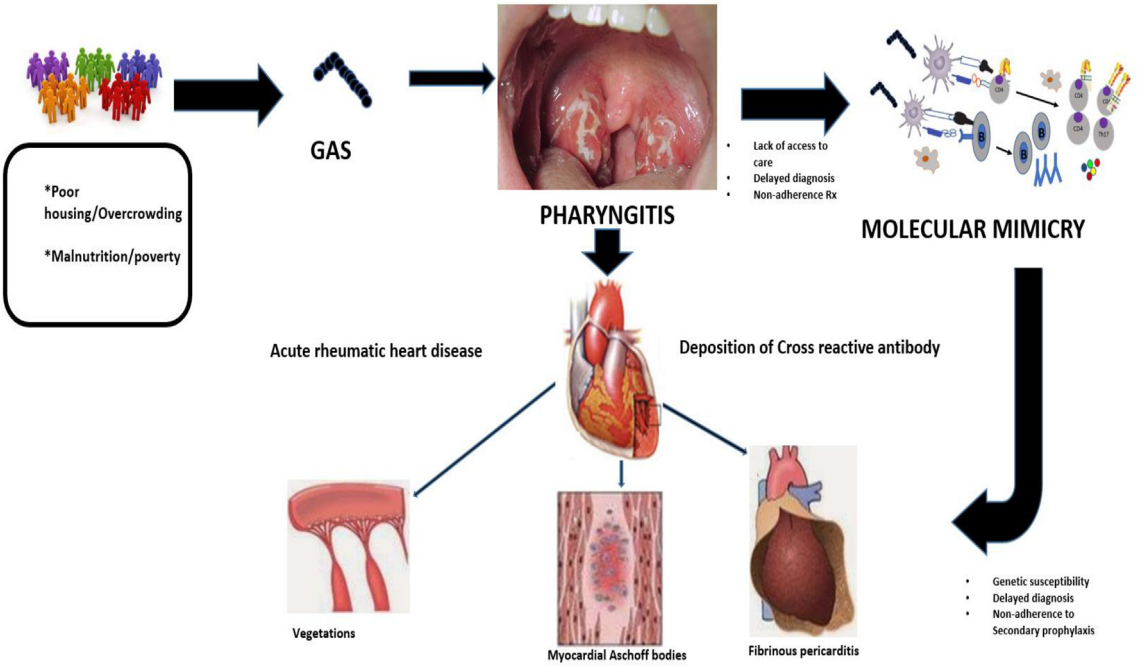

Fig. 1. Pathophysiology of RHD. Environmental factors such as overcrowding, poor housing, poverty and malnutrition predispose people to GAS infection, resulting into pharyngitis. Recurrent pharyngitis leads to acute rheumatic fever, due to molecular mimicry. Untreated acute rheumatic fever results into rheumatic heart disease where the pericardium, myocardium and endocardium are adversely affected thereby leading to fibrinous pericarditis, presence of myocardial Aschoff bodies and valvular vegetations respectively.

adequate information to assess pressure gradients and regurgitant volumes across the valves [18].

2.3. Cardiac computed tomography

Cardiac CT is a diagnostic imaging procedure that uses X-rays to acquire cross-sectional images of the body in different orthogonal planes. Tomograms or slices are reconstructed from the measurements of attenuation coefficients of X-ray beams in the volume of the object studied [17]. The imaging protocol depends on the patient's suspected cardiac lesion, previous repair, age and level of compliance [19]. CT angiography involves contrast material injection, regulated acquisition protocol, ECG-gated multidetector scanner, and modulated radiation dose according to "as low as reasonably achievable" (ALARA) principle [20,21]. Region of interest is monitored by bolus tracking software and scanning triggered when enhancement threshold is reached. The image is reconstructed using maximum intensity projections (MIP), multiplanar reformatting (MPR) and volume rendering techniques (VRT). MPR is commonly used for the evaluation of CT in RHD and other valvular diseases [22]. CT provides incremental information on valvular integrity, mobility and para-valvular pathology [23].

2.4. Cardiac catheterisation and invasive angiography

Cardiac catheterisation is an invasive imaging modality that assesses blood flow and pressures in different chambers and vessels and across the valves. Cardiac catheterisation involves the insertion of catheter into the coronary arteries and/or heart chambers via peripheral arteries and veins. Cardiac catheterisation for haemodynamic assessment is recommended in symptomatic patients when noninvasive tests are equivocal regarding severity of the valve lesion [14]. Cardiac catheterisation may also be used to establish severity of chronic secondary mitral regurgitation (MR) (stages B to D) [14]. Right heart catheterisation estimates pulmonary capillary wedge pressure (PCWP) and pulmonary artery pressure. Further, oximetric studies assess the cardiac output using Fick's principle. To evaluate rheumatic mitral stenosis, valve area is calculated using the Gorlin formula, which requires simultaneous left atrial and ventricular pressure trace. Direct recording of the gradient across the valve and visual classification scale estimates rheumatic aortic stenosis severity [24].

2.5. Cinefluoroscopy

Cinefluoroscopy (CF) is a non-invasive, and readily available imaging technique, which can be performed rapidly in unstable patients with stuck valves. CF allows direct visualisation of the disks and opening and closing angles of bileaflet valves using tangential views. In cases of prosthetic valve obstruction and abnormal valve motion, CF is used to complement echocardiography [25]. CF detected dehiscence/rocking motion of a prosthetic aortic valve in 42 year old RHD patient [26]. Also, CF and TTE showed prosthetic dysfunction (leaflet immobility) secondary to a large thrombus in a 53-year-old RHD patient [27]. Further, the 2017 American College of Cardiology (ACC) recommends CT as a guide for surgical valve replacement [28]. Imaging modalities that may be utilised or recommended in diagnosing RHD are summarised in Table 2.

Table 2
Multi-imaging modalities in RHD.

Cardiac parameters	Echo	CCT	CMR	Fluoroscopy
Anatomy	+++	+++	+++	++
Volume and functions	+++	++	+++	++
Perfusion	++	+	+++	_
Valves	++	++	+++	+
Coronary lumen/wall	++	++	++	++
Coronary blood flow	++	+++	+++	+++
Inflammation	+++	++	+++	_
Fibrosis	+	_	+++	_
Oedema	+	+	+++	_

−, not useful; +, possibly useful; ++, useful, to be considered; +++, very useful, recommended; Echo, Echocardiography, CCT, cardiac computed tomography, CMR, magnetic resonance.

3. Valve lesions

3.1. Mitral regurgitation

Mitral regurgitation (MR) is classified as primary (degenerative) when valvular incompetence results from a pathological abnormality of one or more components of the mitral valve (MV) apparatus. Secondary (functional) MR occurs in the setting of LV remodeling that results in failure of leaflet coaptation in the absence of primary abnormality of the mitral valve apparatus [26]. Rheumatic MR primarily results from structural modifications that reflect chronic scarring of the mitral valve and mitral valve apparatus. The other cause of functional MR is a left atrial dilatation without LV remodeling [29]. The 2014 AHA/ACC guideline for managing valvular heart disease patients highlighted that decisions regarding surgical treatment of MR should be based on grading of MR severity, symptoms and the remodeling response of the left ventricle (LV) to the MR (Table 3). MR severity is classified into four grades (A-D), based on echocardiographic jet area and length, central jet area to left atrium/atrial (LA) ratio, vena contracta, LV and LA sizes [30], effective regurgitant orifice area (EROA), regurgitant volume and regurgitant fraction. Stage A denotes risk factors for MR are present, but no significant MR is detected. Stage B shows mild to moderate MR which is asymptomatic. Stages C and D correspond to severe MR without and with symptoms, respectively [14].

3.1.1. Echocardiography for MR

Valvular thickening occurs in about 56–100% of patients with rheumatic carditis (Fig. 2) [15]. The thickening is mostly located at the free edge of the valve leaflets, where the chordae structures fuse with the leaflet tips, although nodularity is also seen along the length of the leaflet. The 2012 World Health Organization (WHO) classification criteria for abnormally thickened valves include chordal thickening and an objective measurement of the MV without harmonic imaging [31].

TTE and TOE are the main modalities for assessing MR, with the aim of defining the cause of MR (ischaemic or nonischaemic), mechanism (using the Carpentier classification), extent of calcification and the localisation of lesion (using either the Carpentier or Duran nomenclature for scallops) [32]. TOE offers better imaging quality and significant information such as assessment of the vena contracta (VC), distal jet area and ratio, and flow convergence analysis which calculates the proximal isovelocity surface area (PISA) by using colour flow Doppler to measure the EROA [33]. Severe MR is indicated as a distal jet area > 40% of LA area [12]. The method has been shown to be highly sensitive and specific [34] but is limited by underestimation of the severity of eccentric jets [14]. However, vena contracta jet is measured at the regurgitant orifice in the LA in the parasternal long-axis view, in order to avoid overestimation. Regardless of aetiology or jet eccentricity, measurement of this portion by TOE accurately predicts MR severity when compared

Table 3
Classification of chronic MR severity.

Parameters	Mild	Moderate	Severe
EROA, 2D PISA (cm^2)	<0.2	0.2–0.39	>4.0
RVol (mL)	<30	30–59	≥60
RF (%)	<30	30–49	≥50

EROA-Effective Regurgitant orifice area; RVol-Regurgitant volume; RF-Regurgitant fraction; PISA-Proximal isovelocity surface area [17].

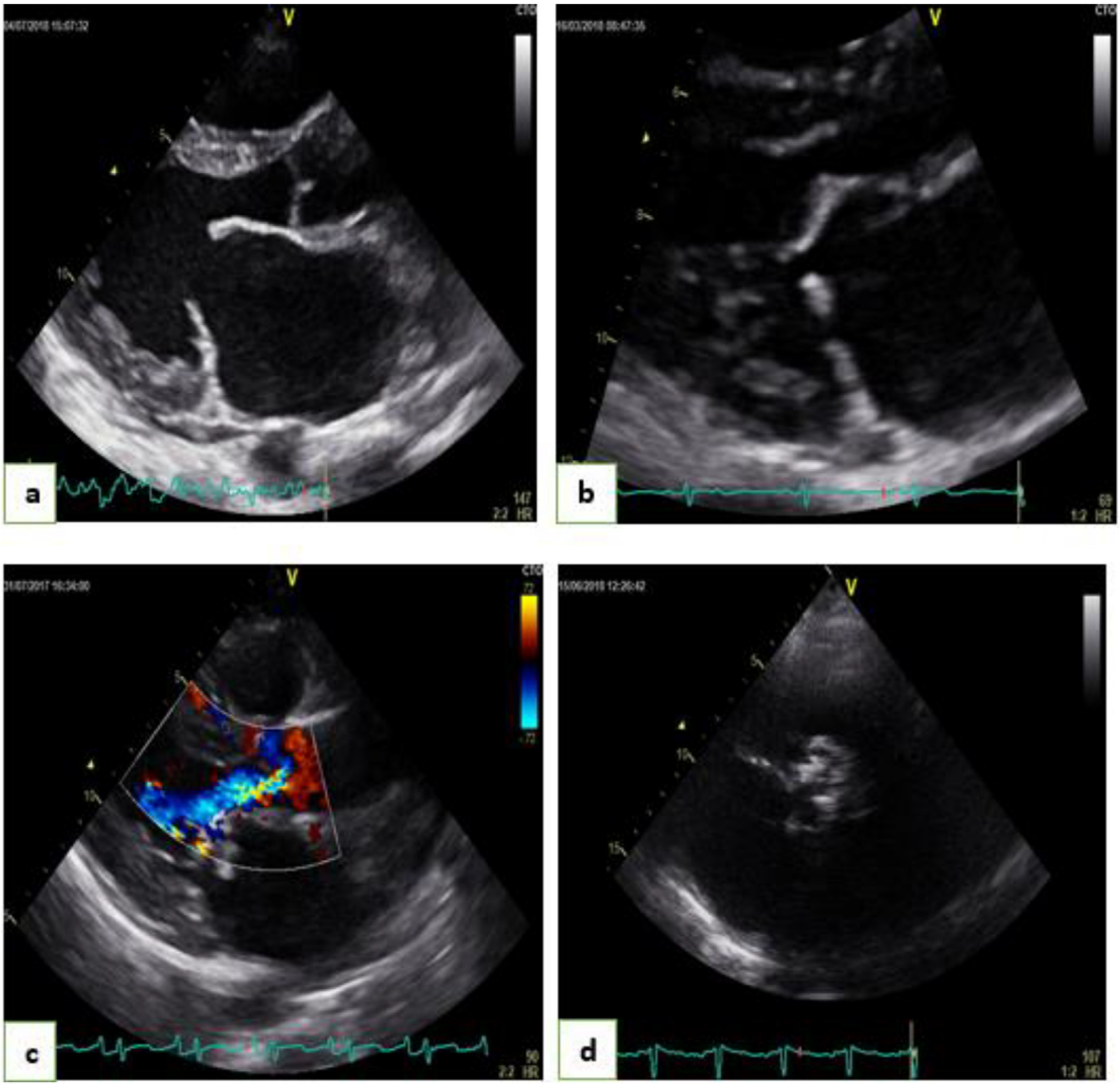

Fig. 2. Echocardiographic images of an RHD patient with multiple valvular lesions. Panels illustrate a 2D echocardiographic images of (a) a regurgitant mitral valve with thickened mitral valve leaflets (b) stenosed mitral valve with a diameter of <1.0 cm. Colour Doppler echocardiographic image revealing (c) aortic regurgitation with Doppler beam revealing the severity of regurgitation across the valve (d) shows aortic stenosis (Note the narrowed and incomplete opening of the valve).

to angiography. VC width of ≥0.7 cm indicates severe MR [35]. Three-dimensional (3D) echocardiography may improve the specificity and sensitivity of RHD detection in mild valvular involvement and facilitate improved surgical preparation for patients with advanced disease [36].

3.1.2. Cardiovascular magnetic resonance for MR

AHA/ACC guidelines have recommended the use of CMR for the assessment of MR severity when TTE is technically limited. CMR is well established for confirming MV morphology and pathology in MR [37–39]. Kon et al demonstrated the use of a combination of CMR velocity-encoded and cine SSFP sequences in quantifying MR severity [40]. CMR is accurate for quantification of MR severity, when compared with 2D echocardiography and has no systematic overestimation [41,42]. Although CMR balanced SSFP sequences provide information about anatomy of the MV, gradient echo cine pulse sequences are more useful for localisation and sizing of regurgitant jets [42]. There are inconsistent reports on semi-quantitative assessment of MR jets by visualisation and/or depth of penetration of MR into the LA on CMR [43,44]. CMR assessment of severity of MR is done by either calculating the regurgitant volume (using the difference between RV and LV volumes), or calculated as the difference between LV stroke volume (SV) and aortic outflow SV [44]. Regurgitant fraction is calculated as the ratio of regurgitant volume to the LV stroke volume, and a regurgitant fraction>48% indicates severe MR [45].

3.1.3. Computed tomography for MR

Multislice CT has also been demonstrated to be accurate for quantitative analysis and in pre-operative planning for percutaneous valve repair [46,47]. Kim et al demonstrated the ability of CT to sufficiently diagnose MV anatomy and geometry pre- and post-operatively, regardless of the surgical method (plasty or replacement). In MV repair, CT can provide detailed structural information including valvular thickening, calcification, sub-valvular structures (such as papillary muscle) and ventricular cavity, and annular stenosis with fibrosis [48]. CT provides accurate characterisation of sub-valvular apparatus and MV geometry [49]. In MR, CT angiography accurately measures the mean regurgitant orifice area, direct features of the MV leaflets (morphology, thickening and calcification), chordae tendinae, papillary muscle and the secondary imaging manifestations such as compensatory LA and/or LV dilatation, and pulmonary congestion [50]. CT is, however, limited in the evaluation of MR as the primary indicator due to the use of radiation and iodine-based contrast [51].

3.1.4. Cardiac catheterisation and invasive angiography for mitral regurgitation

Invasive angiographic procedures begin with fluoroscopy and pose minimal adverse effects of radiation exposure [52]. A typical fluoroscopic study uses about 0.001–0.05 rad of radiation, and dosage depends on fluoroscopic time. Fluoroscopy guides interventional procedures and is useful in assessing the disc mobility of mechanical valves and for percutaneous transvenous mitral commissurotomy in symptomatic patients with valvular dysfunction [52]. Real–time 3D cardiac CT-fluoroscopy fusion imaging guided a transapical implantation of a transcatheter aortic valve prosthesis into a mitral annuloplastic ring [53].

3.2. Mitral stenosis

Mitral stenosis (MS), characterised by a restriction of blood flow from the LA to the LV as a result of a narrowed mitral passage, is often due to RHD [54]. MS occurs more commonly in women than men [55], and may be complicated by mitral annular calcification (MAC) in aged patients, which has also been noted in younger persons residing in LMICs [54]. Other causes of MS include congenital anomalies, prior exposure to chest radiation and mucopolysaccharidosis [54]. Rheumatic MS is often characterised by leaflet commissural fusion, resulting in limited mobility and/or immobility of the posterior leaflet and doming of the anterior leaflet of the MV [44]. Although MS is usually asymptomatic for years, when the mitral orifice is reduced to about a third of its normal size, symptoms associated with left-sided heart failure such as orthopnoea, dyspnoea and paroxysmal nocturnal dyspnoea develop. Chronic MS often results in pulmonary arterial hypertension from pulmonary arteriolar vasoconstriction, intima hyperplasia and medial hypertrophy; secondary obstruction may also develop at the level of the pulmonary veins. Due to both structural and electrical remodeling of the LA, chronic severe MS is often associated with atrial fibrillation. Severity of MS is classified as shown in Table 4.

3.2.1. Echocardiography for MS

Echocardiography, in particular, Doppler TTE, remains the most robust tool for confirming the diagnosis, quantifying MS severity and determining the optimal timing for intervention [44,56,57]. Typical features of MS as revealed by TTE include scarring and thickening of the MV cusps; enlargement of the LA (with a normal LV size); and increased mean pressure gradient across the mitral orifice [58,59]. MVA predicts MS severity using modified Bernoulli equation which calculates mean gradient and pressure half time [60]. Morphological evaluation of MS is important for choice of intervention; identifying MS that is amenable to percutaneous balloon commissurotomy [61].

3.2.2. Cardiovascular magnetic resonance for MS

Although CMR has been reported to diagnose (Fig. 3) and perform planimetry of the mitral orifice and pressure half-time assessment, it may miscalculate MS severity due to overestimation of the mitral valve area. [62] Newer CMR sequences that incorporate mitral annular tracking devices may resolve this problem [63]. CMR measurements of peak volume sweep rates in early diastole (PSRE) and atrial systole (PSRA), PSRE/PSRA ratio, deceleration time of sweep volume (DTSV), and 50% diastolic sweep volume recovery time (DSVRT50) showed a good correlation when compared to TTE diastolic measurements [64]. Feature-tracking CMR not only provided motion and strain quantification using SSFP imaging, [65] but also showed excellent intra- and inter-observer variability [66].

Table 4
Classification of chronic MS severity.

Parameters	Mild	Moderate	Severe
Specific findings Valve Area (cm^2)	>1.5	.0–1.5	<1.0
Supportive findings Mean gradient (mmHg)	<5	5–10	>10
Pulmonary artery pressure (mmHg)	<5	30–50	>50

At heart rates between 60 and 80 bpm and in sinus rhythm.MS, mitral severity. Normal MV area is 4.0–5.0 cm2 [42].

3.2.3. Computed tomography for MS

CT has been reported to accurately assess MV calcification consistently better than echocardiography and CMR and may be useful in quantifying MS severity. Further, CT offers exceptional visualisation of mitral valve morphology and thickening [50]. Additionally, CT may be used to confirm diagnosis of atrial calcification in patients with MS whenever chest radiograph is suboptimal [52,53]. However, CT is not routinely recommended in the evaluation of MS because of radiation exposure and use of iodinated contrast [21,67] whereas echocardiography has gained widespread use owing to its portability and no associated use of radiation [68].

3.2.4. Cardiac catheterisation and invasive angiography for MS

Cardiac catheterisation can be used for MS assessment when there is discordance between clinical and echocardiography findings (Fig. 4–5) [14]. Additionally, invasive measurements are used simultaneously with echocardiography to monitor haemodynamics during a balloon mitral valvuloplasty, allowing an accurate quantification of intracardiac mitral valve pressure gradient and MS severity [69]. MS severity is measured at diastole by simultaneous comparison of the LV pressure and LA pressure [60]. Despite the ability of 3D echocardiography to adequately assess MS severity by MVA planimetry, cardiac catheterisation for LA to LV end-diastolic pressure gradient and MVA by Gorlin's equation can be used [60].

3.3. Aortic regurgitation

Aortic regurgitation (AR) is commonly seen in combination with MR, in rheumatic MV pathology and is commonly classified using Carpentier classification [3]. AR may be caused by the pathology of the leaflets (rheumatic, degenerative, congenital, and/or bicuspid), dilation of the root, aortic dissection or a combination of the three, and iatrogenic complications of aortic valve surgical procedure [30,70–72]. AR creates volume overload and afterload resulting in significant eccentric hypertrophy. Rheumatic AR has a global prevalence of 0.5% of acquired cardiovascular diseases, and incidence increases with age, typically peaking in the 4th to 6th decades of life [30]. The pathological mechanism of rheumatic AR is associated with restricted aortic leaflet motion, a consequence of retracted and thickened aortic leaflet. In RHD, irregular and nodular aortic valve thickening results in a central coaptation defect [73].

3.3.1. Echocardiography for AR

Echocardiography remains the mainstay in the establishment of cause, mechanism and assessment of AR severity (Table 5), and its repercussions on LV function and pulmonary arterial circulation [72]. However, CT and CMR are emerging as important imaging tools that provide additional details about valvular function, structure, and anatomic information of the coronary arteries and ascending thoracic aorta [73].

3.3.2. Computed tomography for AR

CT diagnoses aortic regurgitation in the end-diastolic phase due to insufficient coaptation of aortic valve leaflets. Hence, valvular leakage remains pathognomonic and a diagnostic standard for AR [74]. A significant correlation exists between maximum regurgitant orifice area (ROA) measured with CT and semi-quantitative parameters measured

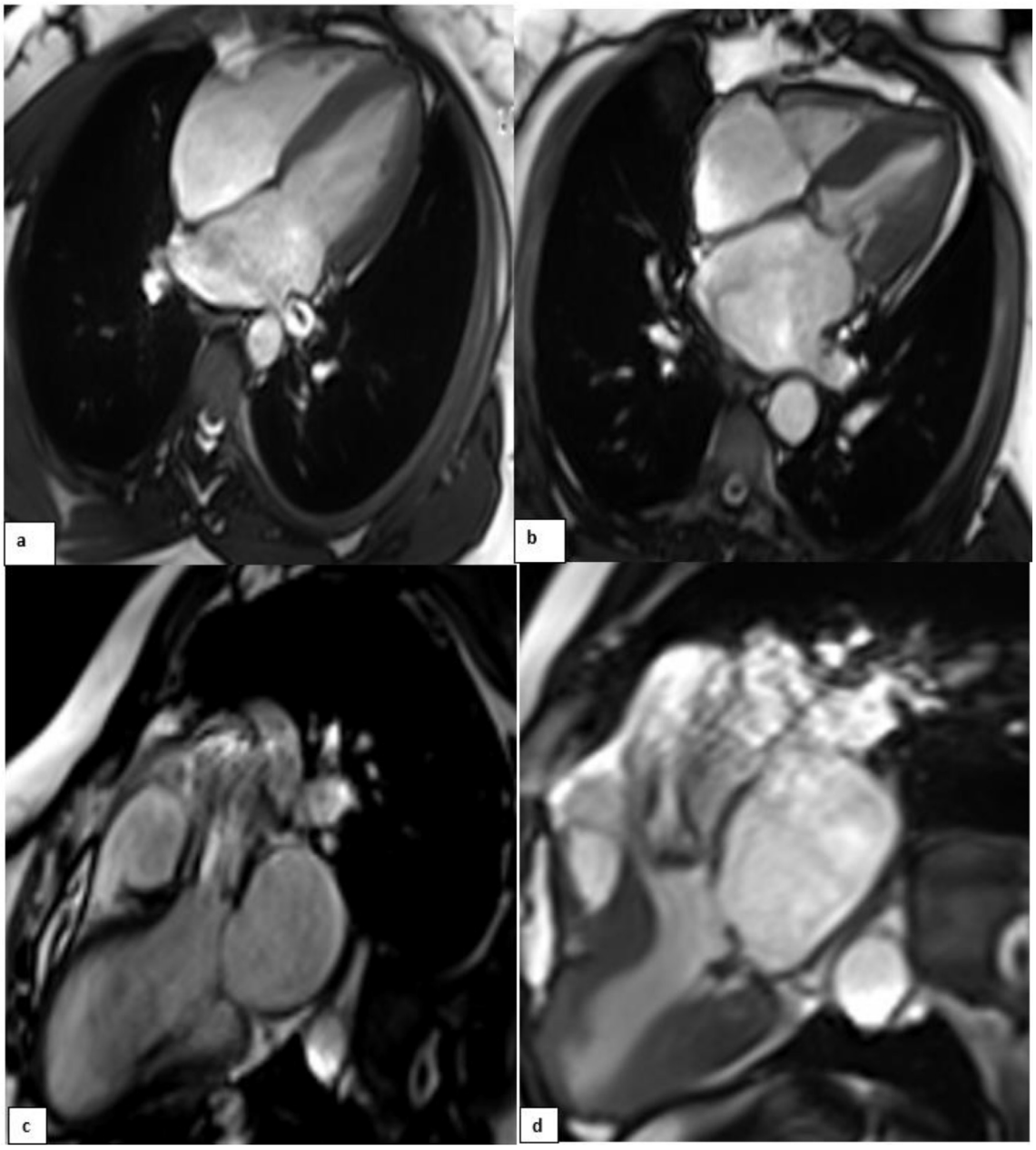

Fig. 3. CMR images of a RHD patient with valvular lesions. Cine MRI in 4-chamber view (a) shows mitral valve incompetence with a backward blood flow into the LV (b) mitral stenosis with a fish-mouth appearance and thickened anterior and posterior mitral valve leaflets. B-SSFP in 3-chamber view (c) aortic regurgitation with a flow acceleration jet across the valve (d) aortic stenosis, white arrows showing the thickened, calcified valve leaflets with incomplete opening of the valve.

with TTE [19,75,76]. Almolla et al demonstrated that 25% of patients with AR had noncoaptated leaflets and increased aortic valvular area (AVA) [77].

3.3.3. Cineangiography for AR

Cineangiography uses the principle of relative density of contrast media in the LV to classify AR severity into 4 grades based on regurgitant volume indices. Unfortunately, cineangiography is limited by its invasiveness, exposure to ionising radiation, volume of injected contrast medium, type and position of catheter tips and other technical factors. Use of qualitative densitometry is highly reproducible in quantifying AR by comparing the density of the contrast in the aorta with that in the LV [78].

3.3.4. Cardiovascular magnetic resonance for AR

CMR may be used to assess the consequences of AR on LV volumes using standard cine sequences. Phase contrast CMR is commonly used to assess haemodynamics of AR, including regurgitant volumes and fraction, as well as to visualise the regurgitant jet. Phase contrast CMR can directly quantify regurgitant volumes and quantify response to volume overload, as opposed echocardiography which secondarily estimates severity using indices such as vena contracta or proximal isovelocity surface area. A potential role of CMR for risk stratification of patients with asymptomatic moderate or severe AR has been proposed [79,80]. Echocardiography and CMR are equivalent in the assessment of LV mass [81]. Quantitative CMR is potentially useful in supplementing echocardiography for management decisions in patients with AR [82].

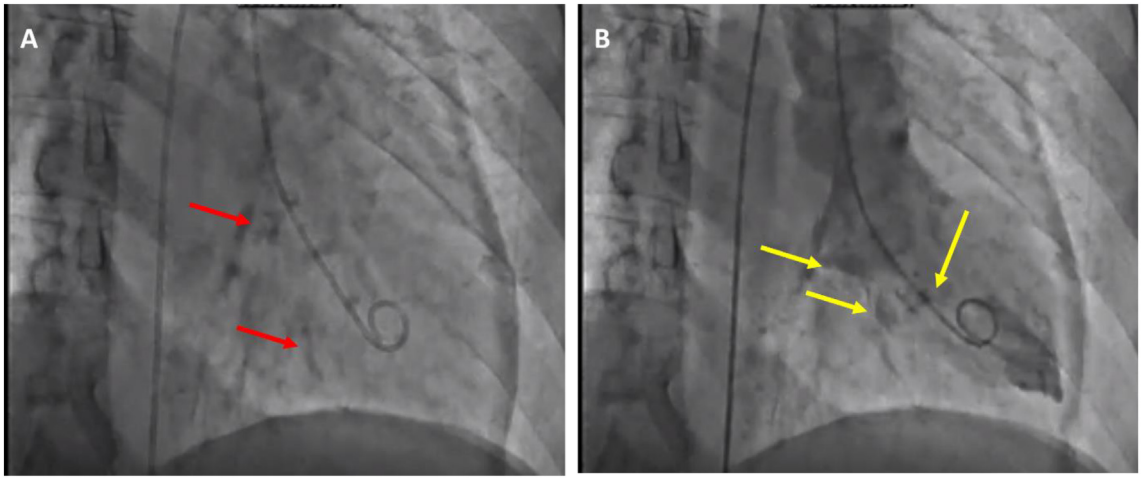

Fig. 4. Invasive catheterisation images of an RHD patient with severe mitral stenosis showing (a) severe mitral annular calcification (red arrows) in diastole and (b) typical restriction of the thickened mitral valve leaflets in systole as well as abnormally contracted and calcific subvalvular apparatus (yellow arrows). (For interpretation of the references to colour in this figure legend, the reader is referred to the web version of this article.)

3.4. Aortic stenosis

Imaging modalities involved in the assessment of aortic stenosis include Doppler echocardiography, TTE, TOE, CMR and CT. While Doppler echocardiography remains the primary imaging modality for evaluating aortic valve morphology and severity of stenosis, TTE can sufficiently assess aortic valve phenotype and the presence of valve calcification. However, TOE, CMR and CT may complement TTE when results are suboptimal, especially in differentiating bicuspid from tricuspid valve in patients with poor image quality, and severe aortic valve calcification. Parameters including peak aortic jet velocity (V_{peak}), mean transvalvular gradients calculated by Bernoulli formula and AVA calculated by continuity equation are employed in assessing the severity of stenosis [72]. Aortic stenosis may be suspected to be severe despite a low gradient [83]. Additionally, when comparing a semi-automated analysis of phase-contrast CMR with Doppler echocardiography in the assessment of aortic valve stenosis, CMR provided an accurate and reproducible result [84]. Phase-contrast CMR is a reliable and user-friendly tool in evaluating stenotic aortic valves [85].

Table 5
Classification of chronic AR severity.

Parameters	Mild	Moderate	Severe
Semi-quantitative			
VCW (cm)	<0.3	0.3–0.6	>0.6
Jet width/LVOT width, central jets (%)	<25	25–64	≥65
Jet CSA/LVOT CSA, central jets (%)	<5	5–59	≥60
Quantitative			
RVol (mL/beat)	<30	30–59	≥60
RF (%)	<30	30–49	≥50
EROA (cm^2)	<0.10	0.10–0.29	≥0.30

CSA-Cross sectional area, VCW-Vena contracta width [71].

3.4.1. Echocardiography for AS

Echocardiography confirms the presence and severity of aortic stenosis (Table 6), by assessing the degree of valvular calcification, LV

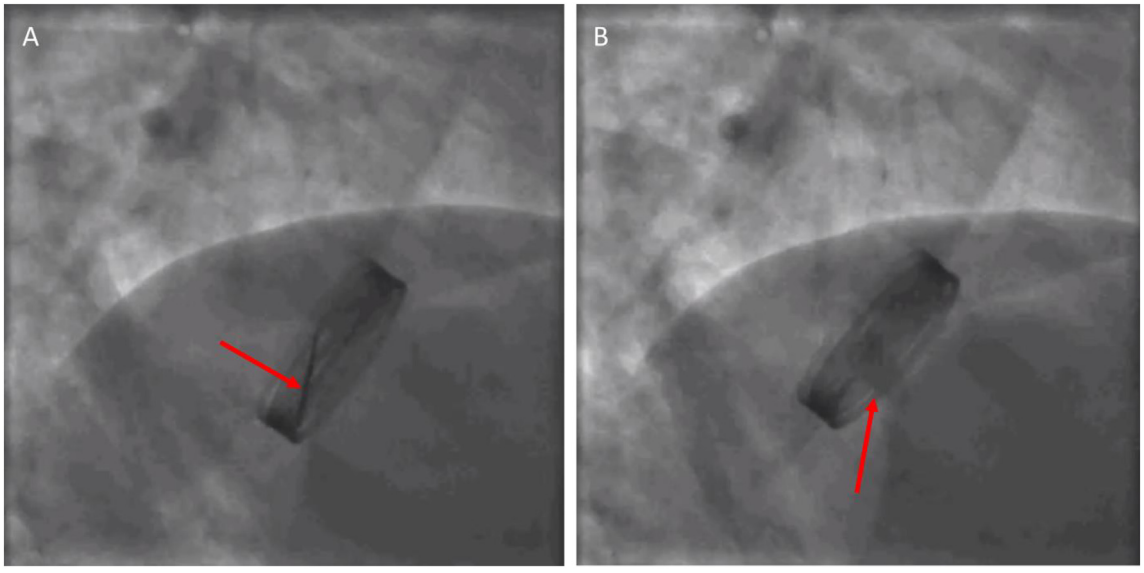

Fig. 5. Patient with prosthetic bileaflet mitral valve with one leaflet stuck. Excursion is noted with the normal leaflet positioned in diastole (a) and in peak systole (b), indicated with red arrows. (For interpretation of the references to colour in this figure legend, the reader is referred to the web version of this article.)

Table 6
Classification of AS severity.

Parameters	Mild	Moderate	Severe
Aortic jet velocity (m/s)	2.6–2.9	3.0–4.0	>4.0
Mean gradient (mmHg)	<20	20–40	>40
AVA (cm^2)	>1.5	1.0–1.5	<1.0
Indexed AVA (cm^2/m^2)	>0.85	0.60–0.85	<0.6
Velocity ratio	>0.5	0.25–0.50	<0.25

ESC Guidelines, AHA/ACC Guidelines [85].

function and LV wall thickness [86]. Doppler echocardiography is the standard technique for assessing aortic stenosis severity. Aortic stenosis may be classified based on peak velocity, maximum/peak pressure gradient, planimetric calculation of the valve area or spectral Doppler recordings combined with the width of LV outflow tract [15].

3.4.2. Computed tomography for AS

Multislice computed tomography (CT) provides important complementary information in the anatomical images of the aortic root and valvular orifice in patients with AS [87]. CT offers adequate quantification of calcium load at the valve level using Agatston score, which has shown good correlation with echocardiography in predicting disease progression [88].

3.4.3. Cardiovascular magnetic resonance for AS

CMR is commonly used in tracking asymptomatic patients with severe AS, assessing reduced LVEF before referral for surgery [30]. Similar to echocardiography, CMR provides reliable information regarding flow and velocity across stenotic or regurgitant valves. Using steady-state free precession (SSFP) sequences, CMR planimetry can measure the anatomical AVA based on direct visualisation of the valve orifice [30]. Late gadolinium enhancement (LGE)-CMR plays a key role in predicting patients' eligibility for transcatheter aortic valve replacement [89].

4. Take home message

Cardiovascular multimodality imaging approach aids in diagnosis, procedural planning, and monitoring patient's outcomes. Most of the current imaging modalities are available, increasingly affordable, and reproducible in assessing RHD. In this article, we have presented the strengths and limitations of multimodality imaging in diagnosis of RHD.

5. Conclusions

Echocardiography is first-line imaging modality for diagnosing rheumatic valvular heart disease due to its ease of use and widespread availability. CMR, CT and invasive angiography are second-line modalities and play a complementary role when echocardiography is suboptimal or equivocal. The use of CT for many valvular applications is limited by high radiation doses, although CT is accompanied by some disadvantages.

Acknowledgement of grant support

Prof. Ntusi gratefully acknowledges support from the South African Medical Research Council, National Research Foundation and the Lily and Ernst Hausmann Trust. This research has been supported by the National Research Foundation (NRF) of South Africa (Grant Nos. 104839 and 105858). Opinions expressed and conclusions arrived at are those of the authors and are not necessarily to be attributed to the funders.

Declaration of competing interest

The Authors declare that there is no conflict of interest.

References

[1] D. Sika-Paotonu, A. Beaton, A. Raghu, A. Steer, J. Carapetis, Acute rheumatic fever and rheumatic heart disease, Nat. Rev. Dis. Prim. 2 (2016) 15085.
[2] A. Prasad, S. Kumar, B. Kr Singh, N. Kumari, Mortality due to rheumatic heart disease in developing world: a preventable problem, J. Clin. Exp. Cardiolog. 08 (2017) 8–11.
[3] L.J. Zühlke, M.E. Engel, D. Watkins, B.M. Mayosi, Incidence, prevalence and outcome of rheumatic heart disease in South Africa: a systematic review of contemporary studies, Int. J. Cardiol. 199 (2015) 375–383.
[4] S. Mendis, P. Puska, B. Norrving (Eds.),Global Atlas on Cardiovascular Disease Prevention and Control, 2011.
[5] J.R. Carapetis, A.C. Steer, E.K. Mulholland, M. Weber, The global burden of group A streptococcal diseases, Lancet Infect. Dis. 5 (2005) 685–694.
[6] E. Marijon, M. Mirabel, D.S. Celermajer, X. Jouven, Rheumatic heart disease, Lancet 379 (2012) 953–964.
[7] Z.M. Makrexeni, L. Pepeta, Clinical presentation and outcomes of patients with acute rheumatic fever and rheumatic heart disease seen at a tertiary hospital setting in Port Elizabeth, South Africa, Cardiovasc. J. Afr. 28 (2017) 1–7.
[8] P.A. Bryant, R. Robins-Browne, J.R. Carapetis, N. Curtis, Some of the people, some of the time susceptibility to acute rheumatic fever, Circulation 119 (2009) 742–753.
[9] F. Aguilar, H.J. Nesser, F. Faletra, S. De Castro, M. Maron, A.R. Patel, N.G. Pandian, Imaging modalities in valvular heart disease, Curr. Cardiol. Rep. 10 (2008) 98–103.
[10] C. Naoum, P. Blanke, J.L. Cavalcante, J. Leipsic, Cardiac computed tomography and magnetic resonance imaging in the evaluation of mitral and tricuspid valve disease: implications for transcatheter interventions, Circ. Cardiovasc. Imaging 10 (2017) 1–17.
[11] J.B. Chambers, M. Garbi, K. Nieman, S. Myerson, L.A. Pierard, G. Habib, J.L. Zamorano, T. Edvardsen, P. Lancellotti, D.V. Delgado, P.B. Cosyns, P.E. Donal, D.R. Dulgheru, D.M. Galderisi, D.M. Lombardi, D.D. Muraru, D.P. Kauffmann, P.N. Cardim, A.P.K. Haugaa, D.R. Rosenhek, Appropriateness criteria for the use of cardiovascular imaging in heart valve disease in adults: a European Association of Cardiovascular Imaging report of literature review and current practice, Eur. Heart J. Cardiovasc. Imaging 18 (2017) 489–498.
[12] P. Lancellotti, S. Price, T. Edvardsen, B. Cosyns, A.N. Neskovic, R. Dulgheru, F.A. Flachskampf, C. Hassager, A. Pasquet, L. Gargani, M. Galderisi, N. Cardim, K.H. Haugaa, A. Ancion, J. Zamorano, G. Habib, The use of echocardiography in acute cardiovascular care: recommendations of the European Association of Cardiovascular Imaging and the Acute Cardiovascular Care Association, Eur. Heart J. Cardiovasc. Imaging 16 (2015) 119–146.
[13] A. Saxena, L. Zühlke, N. Wilson, Echocardiographic screening for rheumatic heart disease: issues for the cardiology community, Glob. Heart 8 (2013) 197–202.
[14] R.A. Nishimura, C.M. Otto, R.O. Bonow, B.A. Carabello, J.P. Erwin, R.A. Guyton, P.T. O'Gara, C.E. Ruiz, N.J. Skubas, P. Sorajja, T.M. Sundt, J.D. Thomas, 2014 AHA/ACC guideline for the management of patients with valvular heart disease: a report of the American college of cardiology/American heart association task force on practice guidelines, J. Am. Coll. Cardiol. 63 (2014) 1–234.
[15] A. Szyszka, A. Gackowski, P. Gościniak, P. Pysz, E. Płońska-gościniak, B. Lichodziejewska, A. Szyszka, T. Kukulski, J.D. Kasprzak, O. Dzikowska-diduch, A. Gackowski, P. Gościniak, P. Pysz, Z. Gąsior, Echocardiography in adults, J. Ultrason. 19 (2019) 54–61.
[16] N. Ntusi, P. Samuels, S. Moosa, A. Mocumbi, Diagnosing cardiac disease during pregnancy: imaging modalities, Cardiovasc. J. Afr. 27 (2016) 95–103.
[17] D.P. Leong, M.X. Joseph, J.B. Selvanayagam, The evolving role of multimodality imaging in valvular heart disease, Heart. 100 (2014) 336–346.
[18] G.S. Gulsin, A. Singh, G.P. McCann, Cardiovascular magnetic resonance in the evaluation of heart valve disease, BMC Med. Imaging 17 (2017) 1–14.
[19] B. Stinn, P. Stolzmann, J. Fornaro, D. Hibbeln, H. Alkadhi, S. Wildermuth, S. Leschka, Technical principles of computed tomography in patients with congenital heart disease, Insights Imaging 2 (2011) 349–356.
[20] A.V. Ngo, A.J. Winant, E.Y. Lee, G.S. Phillips, Strategies for reducing radiation dose in ct for pediatric patients: how we do it, Semin. Roentgenol. 53 (2018) 124–131.
[21] M.F. Morris, J.J. Maleszewski, R.M. Suri, H.M. Burkhart, T.A. Foley, C.R. Bonnichsen, N.S. Anavekar, P.M. Young, E.E. Williamson, J.F. Glockner, A.A. Philip, CT and MR imaging of the mitral valve:, Radiographics, 30(2010) 1603–1620. [22] C. Zhang, S. Nicolaou, Review of cardiac CT imaging, Eur. Soc. Radiol. (2016) 1–16.
[22] C. Zhang, S. Nicolaou, Review of cardiac CT imaging, Euro. Soc. Radiol. (2016) 1–16.
[23] H. Unal Aksu, S. Gorgulu, M. Diker, O. Celik, H. Aksu, D. Ozturk, A. Kiris, A.K. Kalkan, M. Erturk, I. Bakir, Cardiac computed tomography versus echocardiography in the assessment of Stenotic rheumatic mitral valve, Echocardiography 33 (2016) 346–352.
[24] R. Bansal, N.B. Senguttuvan, G. Karthikeyan, M. Ntsekhe, in: S. Dougherty, J. Carapetis, L. Zühlke, N.B.T.-A.R.F, R.H.D. Wilson (Eds.), Chapter 7 - catheter-based evaluation and treatment of rheumatic heart disease, Elsevier, San Diego (CA) 2021, pp. 133–146.
[25] M.O. Gürsoy, M. Kalçık, M. Yesin, S. Karakoyun, E. Bayam, S. Gündüz, M. Özkan, A global perspective on mechanical prosthetic heart valve thrombosis: diagnostic and therapeutic challenges, Anatol. J. Cardiol. 16 (2016) 980–989.
[26] P. Shinde, J. Navale, R. Chavan, M. Shah, A. Chaurasia, D. Nalawade, N. Borikar, IHJ Cardiovascular Case Reports (CVCR) Rocking motion of prosthetic aortic valve on cine fl uoroscopy e a summon of catastrophe, IHJ Cardiovasc. Case Rep. 2 (2018) S24–S26.
[27] P.C.G.D. Campos, M.L. Vieira, I. D'Cruz, D. Weiman, Successful thrombectomy of a stuck mechanical prosthetic mitral valve guided by perioperative transesophageal echocardiography and cinefluoroscopy, Einstein, Case Rep. 7 (2009) 99–102.
[28] J.B. Chambers, M. Garbi, K. Nieman, S. Myerson, L.A. Pierard, H. Gilbert, J.L. Zamorano, T. Edvardsen, P. Lancellotti, Appropriateness criteria for the use of

cardiovascular imaging in heart valve disease in adults: a European Association of Cardiovascular Imaging report of literature review and current practice Eur, Heart J. Cardiovasc. Imaging 70 (2017) 489–498.
[29] V.B.J.J. Delgado, Atrial Functional Mitral Regurgitation, 2010 8–10.
[30] W.S. Choo, R.P. Steeds, Cardiac imaging in valvular heart disease, Br. J. Radiol. 84 (2011) S245–S257 Spec No.
[31] B. Reméanyi, N. Wilson, A. Steer, B. Ferreira, J. Kado, K. Kumar, J. Lawrenson, G. Maguire, E. Marijon, M. Mirabel, A.O. Mocumbi, C. Mota, J. Paar, A. Saxena, J. Scheel, J. Stirling, S. Viali, V.I. Balekundri, G. Wheaton, L. Zühlke, J. Carapetis, World Heart Federation criteria for echocardiographic diagnosis of rheumatic heart disease-an evidence-based guideline, Nat. Rev. Cardiol. 9 (2012) 297–309.
[32] J. Jouan, Mitral valve repair over five decades, Ann. Cardiothorac. Surg. 4 (2015) 322–334.
[33] A. Leśniak-Sobelga, E. Wicher-Muniak, M. Kostkiewicz, M. Olszowska, P. Musiałek, P. Klimeczek, P. Banyś, M. Pasowicz, W. Tracz, P. Podolec, Relationship between mitral leaflets angles, left ventricular geometry and mitral deformation indices in patients with ischemic mitral regurgitation: imaging by echocardiography and cardiac magnetic resonance, Int. J. Card. Imaging 28 (2012) 59–67.
[34] W.A. Zoghbi, D. Adams, R.O. Bonow, M. Enriquez-Sarano, E. Foster, P.A. Grayburn, R.T. Hahn, Y. Han, J. Hung, R.M. Lang, S.H. Little, D.J. Shah, S. Shernan, P. Thavendiranathan, J.D. Thomas, N.J. Weissman, Recommendations for noninvasive evaluation of native valvular regurgitation: a report from the american society of echocardiography developed in collaboration with the Society for Cardiovascular Magnetic Resonance, J. Am. Soc. Echocardiogr. 30 (2017) 303–371.
[35] D.M. Dudzinski, J. Hung, Echocardiographic assessment of ischemic mitral regurgitation, Cardiovasc. Ultrasound 12 (2014) 46.
[36] R. Beniwal, M. Bhaya, R.B. Panwar, S. Panwar, A. Singh, Diagnostic criteria in rheumatic heart disease, Glob. Heart 10 (2015) 81–82.
[37] D.J. Pennell, Cardiovascular magnetic resonance, Circulation. 121 (2010) 692–705.
[38] M. Durand, Miranda, Cardiovascular magnetic resonance imaging in valvular heart disease, South African J. Radiol. 20 (2016) (8 pages).
[39] M. Tarkiainen, P. Sipola, M. Jalanko, T. Heliö, M. Laine, V. Järvinen, K. Häyrinen, K. Lauerma, J. Kuusisto, Cardiovascular magnetic resonance of mitral valve length in hypertrophic cardiomyopathy, J. Cardiovasc. Magn. Reson. 18 (2016) 1–10.
[40] M.W.S. Kon, S.G. Myerson, N.E. Moat, D.J. Pennell, Quantification of regurgitant fraction in mitral regurgitation by cardiovascular magnetic resonance: comparison of techniques, J. Heart Valve Dis. 13 (2004) 600–607.
[41] S. Uretsky, L. Gillam, R. Lang, F.A. Chaudhry, E. Argulian, A. Supariwala, S. Gurram, K. Jain, M. Subero, J.J. Jang, R. Cohen, S.D. Wolff, Discordance between echocardiography and MRI in the assessment of mitral regurgitation severity: a prospective multicenter trial, J. Am. Coll. Cardiol. 65 (2015) 1078–1088.
[42] V. Sachdev, H. Hannoush, S. Sidenko, S.G. Saba, P. Sears-Rogan, W.P. Bandettini, A. Brofferio, S.M. Shanbhag, C.L. Brenneman, K.A. Horvath, M.A. Waclawiw, A.E. Arai, Are echocardiography and CMR really discordant in mitral regurgitation? JACC Cardiovasc. Imaging 10 (2017) 823–824.
[43] F. Saremi, C. Hassani, V. Millan-Nunez, D. Sánchez-Quintana, Imaging evaluation of tricuspid valve: analysis of morphology and function with CT and MRI., AJR, Am. J. Roentgenol. 204 (2015) W531–W542.
[44] S.R. Motiwala, F.N. Delling, Assessment of mitral valve disease: a review of imaging modalities, Curr. Treat. Options Cardiovasc. Med. 17 (2015) 1–16.
[45] E.V. Krieger, J. Lee, K.R. Branch, C. Hamilton-Craig, Quantitation of mitral regurgitation with cardiac magnetic resonance imaging: a systematic review, Heart. 102 (2016) 1864–1870.
[46] P. Rajiah, P. Schoenhagen, The role of computed tomography in pre-procedural planning of cardiovascular surgery and intervention, Insights Imaging. 4 (2013) 671–689.
[47] B.S. Ko, J.D. Cameron, I.T. Meredith, S.K. Seneviratne, Deciphering the role of cardiac computed tomography in interventional cardiology, Interv. Cardiol. 4 (2014) 1–19.
[48] J.H. Kim, E.Y. Kim, G.Y. Jin, J.B. Choi, A review of the use of cardiac computed tomography for evaluating the mitral valve before and after mitral valve repair, Korean J. Radiol. 18 (2017) 773–785.
[49] V. Delgado, L.F. Tops, J.D. Schuijf, A. de Roos, J. Brugada, M.J. Schalij, J.D. Thomas, J.J. Bax, Assessment of mitral valve anatomy and geometry with multislice computed tomography, JACC Cardiovasc. Imaging 2 (2009) 556–565.
[50] J.J.-S. Chen, J. Jeudy, E.M. Thorn, C.S. White, Computed tomography assessment of valvular morphology, function, and disease, J. Cardiovasc. Comput. Tomogr. 3 (2009) S47–S56.
[51] J. Sanz, L. Fernández-Friera, M.J. García, Computed tomography evaluation in valvular heart disease, in: M.J. Budoff, J.S. Shinbane (Eds.), Card. CT Imaging Diagnosis Cardiovasc. Dis, Springer London, London 2010, pp. 159–167.
[52] S. Moosa, N.A.B. Ntusi, Role of cardiovascular magnetic resonance in the evaluation of cardiomyopathy, S Afr J Rad. 2 (2016) 1–10.
[53] E. Schulz, A. Tamm, W. Kasper-König, A. Beiras-Fernandez, C.F. Vahl, T. Münzel, R.S. Von Bardeleben, Transapical implantation of a transcatheter aortic valve prosthesis into a mitral annuloplasty ring guided by real-time three-dimensional cardiac computed tomography-fluoroscopy fusion imaging, Eur. Heart J. 39 (2018) 327–328.
[54] K. Maganti, V.H. Rigolin, M.E. Sarano, R.O. Bonow, Valvular heart disease: diagnosis and management, Mayo Clin. Proc. 85 (2010) 483–500.
[55] R.O. Bonow, B.A. Carabello, K. Chatterjee, A.C. de Leon, D.P. Faxon, M.D. Freed, W.H. Gaasch, B.W. Lytle, R.A. Nishimura, P.T. O'Gara, R.A. O'Rourke, C.M. Otto, P.M. Shah, J.S. Shanewise, 2008 Focused update incorporated into the ACC/AHA 2006 Guidelines for the management of patients with valvular heart disease: a report of the American College of Cardiology/American Heart Association Task Force on Practice Guidelines (Writing Committee to revise the 1998 guidelines for the management of patients with valvular heart disease) Endorsed by the Society of Cardiovascular Anesthesiologists, Society for Cardiovascular Angiography and Interventions, and Society of Thoracic Surgeons, Circulation 118 (2008) e523–e661.
[56] T. Shiota, Clinical application of 3-dimensional echocardiography in the USA, Circ. J. 79 (2015) 2287–2298.
[57] S. Jain, S.V. Mankad, Echocardiographic assessment of mitral stenosis, Cardiol. Clin. 31 (2013) 55905.
[58] H. Baumgartner, J. Hung, J. Bermejo, J.B. Chambers, A. Evangelista, B.P. Griffin, B. Iung, C.M. Otto, P.A. Pellikka, M. Quiñones, Echocardiographic assessment of valve stenosis: EAE/ASE Recommendations for Clinical Practice, J. Am. Soc. Echocardiogr. 22 (2009) 1–23.
[59] A.K. Riegel, R. Busch, S. Segal, J.A. Fox, H.K. Eltzschig, S.K. Shernan, Evaluation of transmitral pressure gradients in the intraoperative echocardiographic diagnosis of mitral stenosis after mitral valve repair, PLoS One 6 (2011) 1–8.
[60] A. Venkateshvaran, S. Sola, S.C. Govind, P.K. Dash, B. Barooah, K. Shahgaldi, A. Sahlén, L. Lund, R. Winter, A.I. Nagy, A. Manouras, The impact of arterial load on left ventricular performance: an invasive haemodynamic study in severe mitral stenosis, J. Physiol. 593 (2015) 1901–1912.
[61] N.C. Wunderlich, R. Beigel, R.J. Siegel, Management of mitral stenosis using 2D and 3D echo-doppler imaging, JACC Cardiovasc. Imaging 6 (2013) 1191–1205.
[62] G. Sommer, J. Bremerich, G. Lund, Magnetic resonance imaging in valvular heart disease: clinical application and current role for patient management, J. Magn. Reson. Imaging 35 (2012) 1241–1252.
[63] S.S. Srivatsa, M.D. Taylor, K. Hor, D.A. Collins, M. King-Strunk, R.A. Pelberg, W. Mazur, Liquefaction necrosis of mitral annular calcification (LNMAC): review of pathology, prevalence, imaging and management: proposed diagnostic imaging criteria with detailed multi-modality and MRI image characterization, Int. J. Card. Imaging 28 (2012) 1161–1171.
[64] V. Wu, J.Y. Chyou, S. Chung, S. Bhagavatula, L. Axel, Evaluation of diastolic function by three-dimensional volume tracking of the mitral annulus with cardiovascular magnetic resonance: comparison with tissue Doppler imaging, J. Cardiovasc. Magn. Reson. 16 (2014) 1–14.
[65] S. Leng, S. Zhang, M. Jiang, X. Zhao, R. Wu, J. Allen, B. He, Imaging 4D morphology and dynamics of mitral annulus in humans using cardiac cine MR feature tracking, Sci. Rep. 8 (2018) 1–13.
[66] R.J. Taylor, W.E. Moody, F. Umar, N.C. Edwards, T.J. Taylor, B. Stegemann, J.N. Townend, K.N. Hor, R.P. Steeds, W. Mazur, F. Leyva, Myocardial strain measurement with feature-tracking cardiovascular magnetic resonance: normal values, Eur. Heart J. Cardiovasc. Imaging 16 (2018) 871–881.
[67] J. Beaudoin, W.E. Thai, B. Wai, M.D. Handschumacher, R.A. Levine, Q.A. Truong, Assessment of mitral valve adaptation with gated cardiac computed tomography: validation with three-dimensional echocardiography and mechanistic insight to functional mitral regurgitation, Circ. Cardiovasc. Imaging. 6 (2013) 784–789.
[68] J.Y. Park, T.A. Foley, C.R. Bonnichsen, M.J. Maurer, K.M. Goergen, V.T. Nkomo, M. Enriquez-Sarano, E.E. Williamson, H.I. Michelena, Transthoracic echocardiography versus computed tomography for ascending aortic measurements in patients with bicuspid Aortic valve, J. Am. Soc. Echocardiogr. 30 (2017) 625–635.
[69] Nishimura, et al., AHA/ACC Focused Update of the 2014 AHA/ACC Guideline for the Management of Patients with Valvular Heart Disease, 2017 2017.
[70] V.T. Nkomo, J.M. Gardin, T.N. Skelton, J.S. Gottdiener, C.G. Scott, M. Enriquez-Sarano, Burden of valvular heart diseases: a population-based study, Lancet 368 (2006) 1005–1011.
[71] G.S. Ribeiro, S.Y. Tartof, D.W.S. Oliveira, A.C.S. Guedes, M.G. Reis, L.W. Riley, A.I. Ko, Surgery for valvular heart disease: a population-based study in a Brazilian urban center, PLoS One 7 (2012) 1–7.
[72] R. Capoulade, P. Pibarot, Assessment of aortic valve disease: role of imaging modalities, Curr. Treat. Options Cardiovasc. Med. 17 (2015) 1–17.
[73] S.M. Ko, Aortic valvular heart disease, in: T.-H. Lim (Ed.), Pract. Textb. Card. CT MRI, Springer Berlin Heidelberg, Berlin, Heidelberg 2015, pp. 219–233.
[74] G. Feuchtner, Imaging of cardiac valves by computed tomography, Scientifica (Cairo) 2013 (2013) 1–13.
[75] H. Alkadhi, D. Bettex, S. Wildermuth, B. Baumert, A. Plass, J. Grunenfelder, L. Desbiolles, B. Marincek, T. Boehm, Dynamic cine imaging of the mitral valve with 16-MDCT: a feasibility study, Am. J. Roentgenol. 185 (2005) 636–646.
[76] M. Feuchtner Gudrun, Wolfgang Dichtl, Silvana Müller, Daniel Jodocy, Thomas Schachner, Andrea Klauser, Johannes O. Bonatti, 64-MDCT for Diagnosis of aortic regurgitation in patients referred to CT coronary angiography, Card. Imaging 191 (2008) W1–W7.
[77] R.M. Almolla, M.M. Enaba, H.M. Abdel-Rahman, Pre-procedural multi-slice computed tomography (MSCT) in aortic valve replacement. Important measurements, Egypt. J. Radiol. Nucl. Med. 48 (2017) 365–373.
[78] C.J. Schultz, A. Tzikas, A. Moelker, A. Rossi, R. Nuis, M.M. Geleijnse, N. van Mieghem, G.P. Krestin, P. de Feyter, P.W. Serruys, P.P. de Jaegere, Correlates on MSCT of paravalvular aortic regurgitation after transcatheter aortic valve implantation using the medtronic corevalve prosthesis, Catheter. Cardiovasc. Interv. 78 (2011) 446–455.
[79] S.G. Myerson, J. D'arcy, R. Mohiaddin, J.P. Greenwood, T.D. Karamitsos, J.M. Francis, A.P. Banning, J.P. Christiansen, S. Neubauer, Aortic regurgitation quantification using cardiovascular magnetic resonance: association with clinical outcome, Circulation 126 (2012) 1452–1460.
[80] S.G. Myerson, Heart valve disease: investigation by cardiovascular magnetic resonance, J. Cardiovasc. Magn. Reson. 14 (2012) 7.
[81] A.C. Armstrong, S. Gidding, O. Gjesdal, C. Wu, D.A. Bluemke, J.A.C. Lima, LV mass assessed by echocardiography and CMR, cardiovascular outcomes, and medical practice, JACC Cardiovasc. Imaging 5 (2012) 837 LP – 848.
[82] S. Kutty, K.K. Whitehead, S. Natarajan, M.A. Harris, G. Wernovsky, M.A. Fogel, Qualitative echocardiographic assessment of aortic valve regurgitation with quantitative

cardiac magnetic resonance: a comparative study, Pediatr. Cardiol. 30 (2009) 971–977.

[83] P. Pibarot, J.G. Dumesnil, Aortic stenosis suspected to be severe despite low gradients, Circ. Cardiovasc. Imaging 7 (2014) 545 LP – 551.

[84] C. Defrance, E. Bollache, N. Kachenoura, L. Perdrix, N. Hrynchyshyn, E. Bruguière, A. Redheuil, B. Diebold, E. Mousseaux, Evaluation of aortic valve stenosis using cardiovascular magnetic resonance: comparison of an original semi-automated analysis of phase-contrast-CMR with Doppler echocardiography, Circ. Cardiovasc. Imaging. 5 (2012) 604–612.

[85] K.S. Nayak, J.-F. Nielsen, M.A. Bernstein, M. Markl, P.D. Gatehouse, R.M. Botnar, D. Saloner, C. Lorenz, H. Wen, B.S. Hu, F.H. Epstein, J.N. Oshinski, S.V. Raman, Cardiovascular magnetic resonance phase contrast imaging, J. Cardiovasc. Magn. Reson. 17 (2015) 71.

[86] H. Baumgartner, J. Hung, J. Bermejo, et al., Recommendations on the echocardiographic assessmnet of aortic valve stenosis: a focused update from the European Association of Cardiovascular Imaging and the American Society of Echocardiography, J Am Soc Echocardiogr. 30 (2017) 372–392.

[87] M.M. Izquierdo-gómez, I. Hernández-betancor, J. García-niebla, B. Marí-lópez, I. Laynez-cerdeña, J. Lacalzada-almeida, Valve calcification in aortic stenosis: etiology and diagnostic imaging techniques, Biomed. Res. Int. 2017 (2017) 1–12.

[88] S.J. Cowell, D.E. Newby, J. Burton, A. White, D.B. Northridge, N.A. Boon, J. Reid, Aortic valve calcification on computed tomography predicts the severity of aortic stenosis, Clin. Radiol. 9260 (2003) 712–716.

[89] R. Bing, J.L. Cavalcante, R.J. Everett, M. Clavel, D.E. Newby, M.R. Dweck, Imaging and impact of myocardial fibrosis in aortic stenosis, JACC Cardiovasc. Imaging 12 (2019) 283–296.